

## Natural Organic Matter Removal by Adsorption onto Dual Nanofiber: Effect of Temperature

<sup>1</sup>Muhammad Ali Zulfikar and <sup>2</sup>Muhammad Nasir

<sup>1</sup>Analytical Chemistry Research Group, Bandung Institute of Technology, Bandung, Indonesia

<sup>2</sup>Applied Chemistry Division, Indonesian Institute of Science, Bandung, Indonesia

---

**Abstract:** The removal of Natural Organic Matter (NOM) using dual nanofiber under the influence of temperature has been investigated. Batch adsorption experiments were carried out using NOM as an adsorbate from Rimbo Panjang, Kampar, Riau Province, Indonesia. It was observed that the amount of NOM removed increase with increasing temperature. The adsorption kinetic data of CR on powdered eggshell was well described by a pseudo-second-order model with the kinetic constants in the range of 0.086-0.265 g/mg/min. Thermodynamic parameters data indicated that the NOM removal was non-spontaneous and endothermic under the experimental conditions with the enthalpy ( $\Delta H$ ) and entropy ( $\Delta S$ ) of +27.44 kJ/mol and +71.56 J/mol, respectively whereas activation energy is 14.82 kJ/mol.

**Key words:** Adsorbent, dual nanofiber, removal, natural organic matter, thermodynamic, adsorption

---

### INTRODUCTION

The presence of Natural Organic Matter (NOM) in water sources is an important issue because it affects water quality, such as color, taste and odor. They also tend to react with a variety of oxidants and disinfectants used for the purification of drinking water forming carcinogenic Disinfection by Products (DBPs) such as trihalomethanes and haloacetic acids (Ngah *et al.*, 2011; Wang *et al.*, 2008; Kamari *et al.*, 2009; Hamid *et al.*, 2011; Rojas *et al.*, 2011; Park and Yoon, 2009; Uyguner *et al.*, 2007; Sonea *et al.*, 2010; Sun *et al.*, 2011). In addition, NOM could enhance the transport of some persistent organic pollutants such as Polycyclic Aromatic Hydrocarbons (PAHs) to aquatic organisms (Laak *et al.*, 2009; Wang *et al.*, 2011a). Therefore, the development of technologies to remove NOM from water is of great importance. At present, there are several methods used to remove NOM from water, such as coagulation-flocculation (Rojas *et al.*, 2011; Uyguner *et al.*, 2007; Sun *et al.*, 2011), electrocoagulation processes (Wang *et al.*, 2011b), oxidation (Uyguner *et al.*, 2007), photocatalysis (Sonea *et al.*, 2010) and membrane technology (Hamid *et al.*, 2011; Rojas *et al.*, 2011; Katsoufidou *et al.*, 2010). All of these alternative processes, however, are high operational cost and none of them therefore is considered by industries to be commercially viable because economically unrealistic. Due to its easy to operate and most effective, adsorption has

been considered as one of the most economically promising techniques for the water and wastewater treatments (Reddy *et al.*, 2012). Activated Carbons (ACs) are the most widely used adsorbents for removing contaminants from wastewater because of its extended surface area, microporous structure, high adsorption capacity and high degree of surface reactivity (Malik, 2003; Toor and Jin, 2012). However, the major drawback of activated carbon is the high operating cost.

In recent years, polymeric have received a lot of attention as powerful adsorbents because their high specific area and high adsorption capacity. The materials can be made into nanofiber by electrospinning which make it easy for regeneration. The main objective of the present work is to investigate the thermodynamic adsorption of these NOM analogues on dual-nanofiber as an adsorbent.

### MATERIALS AND METHODS

Dual nanofiber composed of Polyvinylidene fluoride (PVDF) and Polymethyl Methacrylate (PMMA) were fabricated by simultaneously electrospinning PVDF and PMMA was obtained from Applied Chemistry Laboratory Indonesian, Institute of Science, Bandung, Indonesia. The NOM sample was obtained from Rimbo Panjang, a sub district of Kampar in Riau Province, Indonesia. The characteristics of NOM sample can be seen in Table 1. Before mixing the NOM sample with adsorbent, its pH

Table 1: The characteristics of nom sample

Parameters	Unit	Results
Color	Pt-Co	545
Organic compounds	mg/L KMnO <sub>4</sub>	295
Conductivity	μS/cm	62
pH	-	4.15
Turbidity	mg/L SiO <sub>2</sub>	7.12
Iron	mg/L	0.28
Manganese	mg/L	0.12
Magnesium	mg/L	5.8

value was adjusted using sodium hydroxide and hydrochloric acid. The pH value was measured using 300 Hanna Instrument pH meter.

The adsorption experiments were carried out in 50 mL flasks immersed in a thermostatic shaker bath (ORBITEK, Chennai India) at 25°, 45°, 65° and 85°C in thermostatic shaker bath for 2, 5, 10, 15, 20, 25, 30, 45, 60, 75, 90, 120 and 180 min. Dual nanofiber samples of 0.05 g were mixed with 50 mL of NOM samples. At the end of the predetermined time interval, the suspension was taken out and the supernatant was centrifugated. The NOM concentration of each solution was determined by spectrophotometer (Shimadzu UV-Vis 1601 Model) at the λ254 nm. The percent of NOM removal from peat water was calculated using the following Eq. 1:

$$\text{Removal (\%)} = \left[ \frac{(C_i - C_e)}{C_i} \right] \times 100\% \quad (1)$$

Where C<sub>i</sub> and C<sub>e</sub> are initial and final concentration of NOM in solution, respectively. The adsorption capacity of an adsorbent at equilibrium with solution volume V (L) was calculated using the following Eq. 2:

$$q_e \text{ (mg.g}^{-1}\text{)} = [(C_i - C_e)/m] \times V \quad (2)$$

Where C<sub>i</sub> and C<sub>e</sub> are the initial and final concentration of NOM in solution, respectively and m is mass of adsorbent (g) used.

## RESULTS AND DISCUSSION

**Effect of temperature and contact time:** The effect of temperature on NOM adsorption onto dual nanofiber at vary contact time is shown in Fig 1. It can be seen that a rapid initial uptake of NOM takes place at the beginning contact time and thereafter, the adsorption increases gradually with increasing contact time and reaches equilibrium after 60 min.

Figure 1 shows the removal of NOM by dual nanofiber was strongly affected by temperature. The removal of NOM increased dramatically with increasing temperature (from 25°-85°C) for the concentrations of NOM considered.

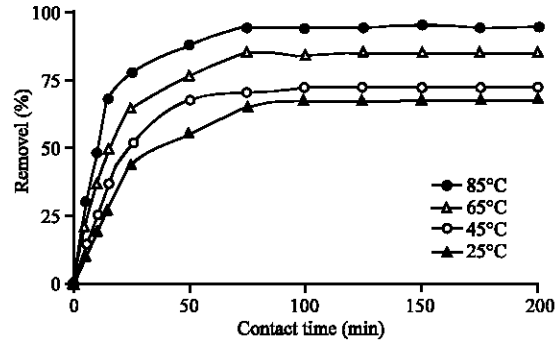


Fig. 1: Effect of temperature on NOM removal

Increasing of temperature is known to increase the diffusion rate of the NOM molecule across the external boundary layer and the internal pores of the adsorbent particles. Furthermore, increasing temperature may produce a swelling effect within the internal structure of the adsorbent enabling large NOM to penetrate further (McKay, 1982; Yoshida *et al.*, 1993; Sarkar and Poddar, 1994; Zulfikar *et al.*, 2015, 2016).

**Adsorption kinetics:** The kinetic adsorption data were evaluated to understand the dynamics of the adsorption reaction in terms of the order of the rate constant. Three kinetic models were applied to the adsorption kinetic data in order to investigate the behaviour of adsorption process of NOM onto the adsorbents. These models include the pseudo-first-order kinetics (reversible or irreversible), the pseudo-second-order and intra-particle-diffusion. The linear form of reversible pseudo-first-order model can be formulated as:

$$\text{Log} (q_e - q_t) = \text{log} q_e - (k_1/2.303) t \quad (3)$$

Where q<sub>e</sub> and q<sub>t</sub> are the amounts of CR adsorbed (mg/g) at equilibrium and at time (t), respectively and k<sub>1</sub> (min<sup>-1</sup>) is the rate constant of this equation. The value of q<sub>e</sub> and k<sub>1</sub> was obtained from intercepts and slope of the linear plots of log (q<sub>e</sub>-q<sub>t</sub>) against t.

Figure 2 shows the kinetics of NOM adsorption by using pseudo-first-order model and its kinetics parameters are shown in Table 2. It was observed that the pseudo-first-order kinetic model did not adequately fit the experimental values. Also from Table 2, it is indicated that the values of the correlation coefficients are not high for the various dye concentrations. Furthermore, a large difference of equilibrium adsorption capacity (q<sub>e</sub>) between the experiment and calculation was observed indicating a poor pseudo first-order fit to the experimental data.

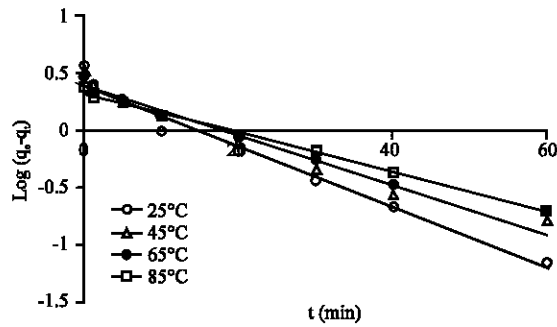


Fig. 2: Pseudo-first-order plot for NOM adsorption

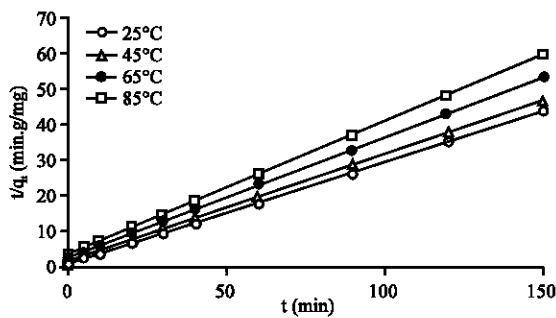


Fig. 3: Pseudo-second-order plot for NOM adsorption

The kinetic data were further analyzed using pseudo second-order kinetics model. This model is based on the assumption of chemisorption of the adsorbate on the adsorbents. This model is given as:

$$t/q_t = 1/k_2 \times q_e^2 + t/q_e \quad (4)$$

Where  $q_e$  and  $q_t$  are the amounts of CR adsorbed (mg/g) on adsorbents at equilibrium and at time  $t$ , respectively and  $k_2$  is the rate constant (g/mg.min).

The linear plots of  $t/q_t$  versus  $t$  show a good agreement with experimental data giving the correlation coefficients close to 1 (Fig. 3). Also, the calculated  $q_2$  values agree very well with the experimental data at all temperature (Table 2). This means that the adsorption system obeys the pseudo-second-order kinetic model for the entire adsorption period, supporting the assumption that the adsorption of NOM on dual nanofiber is mainly chemisorption (Zulfikar *et al.*, 2016; Fan *et al.*, 2011).

Table 2 shows that, the values of the rate constant  $k_2$  increase with increasing temperature. The reason for this behavior can be attributed to the increase in the mobility of NOM molecule with increasing temperature and consequently higher diffusion rates are obtained.

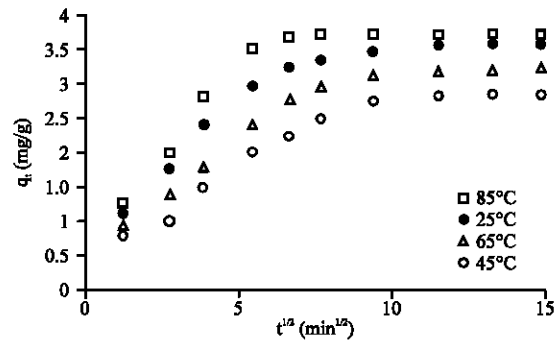


Fig. 4: Intra-particle-diffusion plot for NOM adsorption

Table 2: Thermodynamic parameters of removal process

Temp. (°C)	Pseudo-first-order		Pseudo-second-order		$q_e$ , exp. (mg/g)
	$q_1$ (mg/g)	$k_1$ (min <sup>-1</sup> )	$q_2$ (mg/g)	$k_2$ (g/mg.min)	
25	3.688	0.186	3.866	0.086	3.858
45	3.884	0.182	3.955	0.132	3.914
65	4.024	0.166	4.124	0.186	4.136
85	4.196	0.148	4.185	0.265	4.188

Adsorption kinetics is usually controlled by different mechanisms, the most general of which is the diffusion mechanism. To investigate the mechanism of adsorption, the intra-particle diffusion model is used. The intra-particle diffusion model can be defined as:

$$q_t = k_d \times t^{1/2} + c \quad (5)$$

Where  $k_d$  and  $c$  are intra-particle diffusion rate constant (mg/g.min<sup>0.5</sup>) and a constant, respectively. To follow the intra-particle diffusion model, a plot of  $q_t$  against  $t^{1/2}$  should give a linear line where a slope is  $k_d$  and intercept  $c$ . Values of  $c$  give information regarding the thickness of boundary layer, i.e., the larger intercept the greater is the boundary layer effect (Fan *et al.*, 2011; Lin and Zhan, 2012; Zulfikar *et al.*, 2013; Elkady *et al.*, 2011).

The plot of  $q_t$  against  $t^{1/2}$  using initial kinetic data may be distinguished in two or more steps taking place during adsorption process including instantaneous adsorption stage by external mass transfer (first sharper portion) intra-particle diffusion which is the rate controlling stage (second portion as the gradual adsorption stage) and the final equilibrium stage where the intra-particle diffusion starts to slow down due to the extremely low solute concentration in solution (the third portion) (Fan *et al.*, 2011; Lin and Zhan, 2012; Zulfikar *et al.*, 2013; Elkady *et al.*, 2011).

Figure 4 shows the two straight lines can be diagnosed for four adsorption systems. The first line with steeper slope corresponds to film and pore diffusion taking place simultaneously in the adsorption systems.

The slope of this linear portion can be defined as a rate parameter and characteristic of the rate of adsorption in the region where intra-particle diffusion is occurring. Declining of the second linear portion is dealing with the diminishing of intra-particle diffusion and reaching equilibrium.

**Thermodynamic study:** The Gibbs free energy change ( $\Delta G$ ) during the adsorption process was calculated by the Van't Hoff equations. Where  $R$ ,  $T$  and  $K_L$  are the universal gas constant (8.314 J/mol/K), temperature (K) and langmuir isotherm constant, respectively. The enthalpy change ( $\Delta H$ ) and entropy change ( $\Delta S$ ) during the adsorption process were calculated from the slope and the intercept of the plots of  $\ln K_L$  versus  $1/T$  (Eq. 7):

$$\Delta G^{\circ} = -RT \ln K_L \quad (6)$$

$$\Delta G^{\circ} = H^{\circ} - T \times \Delta S^{\circ} \quad (7)$$

Combining Eq. 3 and 4 and rearranging:

$$\ln K_L = \left[ \left( \Delta S^{\circ} / R \right) - \left( \Delta H^{\circ} / R.T \right) \right] \quad (8)$$

The parameter values obtained from the slope and intercept of the linear plot of  $\ln K_L$  vs.  $1/T$  are tabulated in Table 3. A positive value of  $\Delta S^{\circ}$  indicates that the removal process is endothermic and thus the removal of NOM by dual nanofiber is entropy driven (Zulfikar *et al.*, 2015, 2016; Salman *et al.*, 2007).

The enthalpy change ( $\Delta H^{\circ}$ ) for chemisorption is in the range 40-120 kJ/mol (Zulfikar *et al.*, 2015, 2016; Alkan *et al.*, 2004). Since, the value of  $\Delta H^{\circ}$  observed in the system is lower than 40 kJ/mol, so, the removal of NOM from water using dual nanofiber by physisorption.

The positive values of Gibbs free energy ( $\Delta G^{\circ}$ ) obtained indicate the non-spontaneous nature of adsorption process at the range of temperatures being studied. It can also noted that the value of  $\Delta G^{\circ}$  become more negative with the increase of temperature which indicates that the reaction is more favorable at high temperatures (Table 3).

The other thermodynamic parameter is activation energy ( $E_a$ ). The Arrhenius equation was applied to evaluate the  $E_a$  of the adsorption process:

$$\ln k = \ln A - \frac{E_a}{R.T} \quad (9)$$

Where  $k$  is rate constant of pseudo-second-order kinetic model (g/mg/min),  $E_a$  is the activation energy

Table 3: Thermodynamic parameters of removal process

Thermodynamic parameters				
Temp. (°C)	$\Delta G^{\circ}$ (kJ/mol)	$\Delta H^{\circ}$ (kJ/mol)	$\Delta S^{\circ}$ (J/mol)	$\Delta E_a$ (kJ/mol)
25	3.57	27.44	71.56	14.82
45	2.69			
65	1.96			
85	1.11			

(kJ/mol),  $A$  the Arrhenius factor,  $R$  the gas constant (8.314 J/mol K) and  $T$  is the solution absolute temperature (K). The linear plot of  $\ln k$  versus  $1/T$  gives a straight line with slope  $E_a/R$ . The magnitude of  $E_a$  gives an opinion about the adsorption mechanism (Zulfikar *et al.*, 2016; Fan *et al.*, 2011; Rahchamani *et al.*, 2011; Wang *et al.*, 2013). Physical adsorption typically has activation energy of 5-40 kJ/mol and chemical adsorption has activation energy of 40-800 kJ/mol (Zulfikar *et al.*, 2016; Fan *et al.*, 2011; Rahchamani *et al.*, 2011; Wang *et al.*, 2013). The activation energy obtained in this study is 18.62 kJ/mol (Table 3) indicating that HA adsorption onto the MIPs corresponds to physisorption. The positive value of  $E_a$  suggests that an increase in temperature favors the adsorption of HA on MIPs and the adsorption process is endothermic in nature (Zulfikar *et al.*, 2016; Lin and Zhan, 2012).

## CONCLUSION

The result from this work showed that the temperature has an important role in the removal of NOM by dual nanofiber. Thermodynamic parameters data indicated that the NOM removal process was non-spontaneous and endothermic under the experimental conditions, with the Gibbs free energy ( $\Delta G^{\circ}$ ) in the range of 3.57-1.11 kJ/mol, enthalpy ( $\Delta h^{\circ}$ ) and entropy ( $\Delta s^{\circ}$ ) of 0.27 kJ/mol and 0.71 J/mol, respectively whereas activation energy is 14.82 kJ/mol.

## ACKNOWLEDGEMENT

The researcher is very grateful to Higher Education General for the financial support this research study through Riset Desentralisasi 2016.

## REFERENCES

- Alkan, M., O. Demirbas, S. Celikcapa and M. Dogan, 2004. Sorption of acid red 57 from aqueous solution onto sepiolite. *J. Hazard. Mater.*, 116: 135-145.
- Elkady, M.F., A.M. Ibrahim and M.A. El-Latif, 2011. Assessment of the adsorption kinetics, equilibrium and thermodynamic for the potential removal of reactive red dye using eggshell biocomposite beads. *Desalination*, 278: 412-423.

- Fan, J., W. Cai and J. Yu, 2011. Adsorption of N719 dye on anatase TiO<sub>2</sub> nanoparticles and nanosheets with exposed (001) facets: Equilibrium, kinetic and thermodynamic studies. *Chem. Asian J.*, 6: 2481-2490.
- Hamid, N.A.A., A.F. Ismail, T. Matsuura, A.W. Zularisam, W.J. Lau, E. Yuliwati and M.S. Abdullah, 2011. Morphological and separation performance study of polysulfone/titanium dioxide (PSF/TiO<sub>2</sub>) ultrafiltration membranes for humic acid removal. *Desalination*, 273: 85-92.
- Kamari, A., W.W. Ngah and L.W. Wong, 2009. Shorea dasyphylla sawdust for humic acid sorption. *Eur. J. Wood Wood Prod.*, 67: 417-426.
- Katsoufidou, K.S., D.C. Sioutopoulos, S.G. Yiantsios and A.J. Karabelas, 2010. UF membrane fouling by mixtures of humic acids and sodium alginate: Fouling mechanisms and reversibility. *Desalin.*, 264: 220-227.
- Laak, T.T.L., T.M.A. Bekke and J.L. Hermens, 2009. Dissolved organic matter enhances transport of PAHs to aquatic organisms. *Environ. Sci. Technol.*, 43: 7212-7217.
- Lin, J. and Y. Zhan, 2012. Adsorption of humic acid from aqueous solution onto unmodified and surfactant-modified chitosan-zeolite composites. *Chem. Eng. J.*, 200: 202-213.
- Malik, P.K., 2003. Use of activated carbons prepared from sawdust and rice-husk for adsorption of acid dyes: A case study of acid yellow 36. *Dyes Pigments*, 56: 239-249.
- McKay, G., 1982. Adsorption of dyestuffs from aqueous solutions with activated carbon I: Equilibrium and batch contact-time studies. *J. Chem. Technol. Biotechnol.*, 32: 759-772.
- Ngah, W.S.W., S. Fatinathan and N.A. Yosop, 2011. Isotherm and kinetic studies on the adsorption of humic acid onto chitosan-H<sub>2</sub>SO<sub>4</sub> beads. *Desalination*, 272: 293-300.
- Park, S.J. and T.I. Yoon, 2009. Effects of iron species and inert minerals on coagulation and direct filtration for humic acid removal. *Desalin.*, 239: 146-158.
- Rahchamani, J., H.Z. Mousavi and M. Behzad, 2011. Adsorption of methyl violet from aqueous solution by polyacrylamide as an adsorbent: Isotherm and kinetic studies. *Desalination*, 267: 256-260.
- Reddy, M.C.S., L. Sivaramakrishna and A.V. Reddy, 2012. The use of an agricultural waste material, Jujuba seeds for the removal of anionic dye (Congo red) from aqueous medium. *J. Hazard. Mater.*, 203-204: 118-127.
- Rojas, J.C., J. Perez, G. Garralon, F. Plaza and B. Moreno *et al.*, 2011. Humic acids removal by aerated spiral-wound ultrafiltration membrane combined with coagulation-hydraulic flocculation. *Desalin.*, 266: 128-133.
- Salman, M., B. El-Eswed and F. Khalili, 2007. Adsorption of humic acid on bentonite. *Appl. Clay Sci.*, 38: 51-56.
- Sarkar, M. and S. Poddar, 1994. Study of the adsorption of methyl violet onto fly-ash. *Anal. Proc.*, 31: 213-215.
- Sonea, D., R. Pode, F. Manea, C. Ratiu and C. Lazau *et al.*, 2010. The comparative assessment of photolysis, sorption and photocatalysis processes to humic acids removal from water. *Chem. Bull. Politehnica Univ.*, 55: 148-151.
- Sun, C., Q. Yue, B. Gao, R. Mu and J. Liu *et al.*, 2011. Effect of pH and shear force on flocs characteristics for humic acid removal using polyferric aluminum chloride-organic polymer dual-coagulants. *Desalin.*, 281: 243-247.
- Toor, M. and B. Jin, 2012. Adsorption characteristics, isotherm, kinetics and diffusion of modified natural bentonite for removing diazo dye. *Chem. Eng. J.*, 187: 79-88.
- Uyguner, C.S., S.A. Suphandag, A. Kerc and M. Bekbolet, 2007. Evaluation of adsorption and coagulation characteristics of humic acids preceded by alternative advanced oxidation techniques. *Desalin.*, 210: 183-193.
- Wang, H., A.A. Keller and K.K. Clark, 2011. Natural organic matter removal by adsorption onto magnetic permanently confined micelle arrays. *J. Hazard. Mater.*, 194: 156-161.
- Wang, J., X. Han, H. Ma, Y. Ji and L. Bi, 2011. Adsorptive removal of humic acid from aqueous solution on polyaniline-attapulgite composite. *Chem. Eng. J.*, 173: 171-177.
- Wang, S.G., X.F. Sun, X.W. Liu, W.X. Gong and B.Y. Gao *et al.*, 2008. Chitosan hydrogel beads for fulvic acid adsorption: Behaviors and mechanisms. *Chem. Eng. J.*, 142: 239-247.
- Wang, W., B. Zheng, Z. Deng, Z. Feng and L. Fu, 2013. Kinetics and equilibriums for adsorption of poly(vinyl alcohol) from aqueous solution onto natural bentonite. *Chem. Engine. J.*, 214: 343-354.
- Yoshida, H., A. Okamoto and T. Kataoka, 1993. Adsorption of acid dye on cross-linked chitosan fibers: Equilibria. *Chem. Eng. Sci.*, 48: 2267-2272.
- Zulfikar, M.A., D. Wahyuningrum and S. Lestari, 2013. Adsorption of lignosulfonate compound from aqueous solution onto chitosan-silica beads. *Sep. Sci. Technol.*, 48: 1391-1401.
- Zulfikar, M.A., D. Wahyuningrum, R.R. Mukti and H. Setiyanto, 2016. Molecularly Imprinted Polymers (MIPs): A functional material for removal of humic acid from peat water. *Desalin. Water Treat.*, 57: 15164-15175.
- Zulfikar, M.A., H. Setiyanto, R. Rusnadi and L. Solakhudin, 2015. Rubber seeds (*Hevea brasiliensis*): An adsorbent for adsorption of Congo red from aqueous solution. *Desalin. Water Treat.*, 56: 2976-2987.